DMD Fast Forward. Published on March 11, 2019 as DOI: 10.1124/dmd.118.085209
This article has not been copyedited and formatted. The final version may differ from this version.

DMD # 85209

Title:

A novel depurination methodology to assess DNA alkylation of chloro bis-seco-cyclopropylbenzoindoles (CBIs) allowed for comparison of minor groove reactivity

Authors:

Shuai Wang, Buyun Chen, Peter Dragovich, Thomas Pillow, Leanna Staben, Jun Guo, Dian Su, Chenghong Zhang, Sudheer Bobba, Yong Ma, Jianshuang Wang, Dewakar Sangaraju, BinQing Wei, Gail Lewis Phillips, Cyrus Khojasteh, Donglu Zhang

Affiliations:

Drug Metabolism and Pharmacokinetics (SW, BC, DS, CZ, SB, YM, JW, DS, CK, DZ), Discovery Chemistry (PD, TP, LS, BW), Discovery Biology (JG, GP), Genentech, Inc., South San Francisco, CA 94080, USA

DMD Fast Forward. Published on March 11, 2019 as DOI: 10.1124/dmd.118.085209
This article has not been copyedited and formatted. The final version may differ from this version.

Running Title: Bis-seco-CBI DNA alkylation

Corresponding Author:

Drug Metabolism and Pharmacokinetics, Genentech, Inc., 1 DNA Way, South San Francisco, CA 94080, USA

Tel: 650-467-7255, Email: zhang.donglu@gene.com

Document Statistics:

Text Pages: 46

Tables: 4

Figures: 4

References: 37

Abstract: 250 words

Introduction: 677 words

Materials and Methods: 678 words

Results: 1714 words

Discussion: 1494 words

Key Words: DNA adducts, HPLC, nucleic acids, reactive metabolites/intermediates, antibody-drug conjugates

Abbreviations:

ADC, antibody drug conjugate; CBI, cyclopropyl benzoindole; CPI, cyclopropyl pyrroloindole; DNA, deoxyribonucleic acid; DMR, di- to mono-alkylation ratio; EA, ethyl acetate; LC-MS, liquid chromatography – mass spectrometry; Oligo, oligodeoxyribonucleotide; XIC, extracted ion chromatogram;

DMD Fast Forward. Published on March 11, 2019 as DOI: 10.1124/dmd.118.085209
This article has not been copyedited and formatted. The final version may differ from this version.

Abstract

Duocarmycins (including cyclopropyl pyrroloindole, CPI or cyclopropyl benzoindole, CBI) are a class of DNA minor groove alkylators and seco-CPI/CBIs are synthetic pro-forms that can spirocyclize to CPI/CBI. Bis-CPI/CBIs are potential drug candidates because of their enhanced cytotoxicity from DNA cross-linking, but are difficult to be analyzed for structure-activity correlation because of their DNA reactivity. To study its DNA alkylation, neutral thermal hydrolysis has been frequently applied to process depurination. However, unwanted side reactions under this condition have been reported, which could lead to poor correlation of DNA alkylation data with efficacy results, especially for bis-CPI/CBIs. In this study, an acidic depurination method was developed and applied for analyses of DNA alkylation, and showed to be an easier and milder method than the traditional neutral thermal hydrolysis. DNA alkylation and stability of three bis-seco-CBIs were characterized in comparison with two mono-seco-CPIs. The results suggested that: (1) The acidic depurination method was capable of capturing a more representative population, sometimes a different population, of DNA adducts as they existed on DNA compared to the heat depurination method. (2) Di-adenine adducts were captured as expected for the CBI dimers, while the major type of adducts was still mono-adenine adducts. (3) The rate of DNA alkylation, DNA adduct profile, and relative amounts of di-adduct versus mono-adduct were significantly affected by the size, and possibly lipophilicity of the non-alkylating part of the molecules. (4) Spirocyclization and amide hydrolysis represented two major pathways of degradation. Overall, by applying acidic depurination analyses, this study has illustrated DNA adduct characteristics of novel bis-seco-CBIs with dominating mono-alkylation and provides an alternative method for evaluating DNA minor groove alkylators. These findings provide an effective analytical tool to evaluate DNA alkylators and to study the DNA alkylation that is a disposition mechanism of these compounds.

Introduction

Duocarmycins are a series of compounds first discovered in *Streptomyces* (Yasuzawa et al., 1995). These compounds display picomolar cell killing activities, which are related to their potent sequence selective DNA alkylation (Tichenor et al., 2007; MacMillan and Boger, 2009). The cyclopropyl pyrroloindole (CPI) group in these molecules acts as electrophiles upon binding in the DNA minor groove, favoring the attack of the adenine N3 position (Boger and Johnson, 1995) (Scheme 1). The naturally occurring S conformation is also important, with much higher activity (500 fold) over the R isoforms (Boger and Garbaccio, 1999b; Tietze and von Hof, 2011). Modification of the CPI group by replacing the pyrrole ring with a benzene ring lead to increased stability potentially due to less strain from the ring expansion. Additionally, the resultant cyclopropyl benzoindole (CBI) compounds also displayed more potent DNA alkylation and cytotoxicity (Boger et al., 1991).

Molecules containing two CPI groups were developed to achieve higher potency from intra- and inter-strand DNA cross-linking (Mitchell et al., 1989; Boger et al., 2000). Most notably, bizelesin, a CPI-dimer, was evaluated in a Phase I clinical trial for advanced solid tumors (Schwartz et al., 2003). Mitchell et al. synthesized several CPI dimers and found an optimal chain length of 3 carbons apart with a 2 pM *in vitro* IC_{50} (Mitchell et al., 1989). Jia et al. also reported seco-CBI dimers linked with 3 carbons apart showed the highest *in vitro* potency (Jia and Lown, 2000). Consistent with these findings, bis-seco-CPIs connected by a 3,3'-(1,4-phenylene)diacryloyl group has previously shown superior cytotoxicity with an *in vitro* IC_{50} of 2.7 pg/ml compared to 60 pg/ml of bizelesin, and inhibited xenograft tumor growth at 0.254 µg/kg as compared to 3.72 µg/kg by bizelesin *in vivo* with 4 fold higher therapeutic index (Fukuda et al., 1998). However, these therapeutics inevitably suffer from off-target toxicity and severe side reactions (McGovren et al., 1984; Baraldi et al., 2004).

Antibody drug conjugates (ADC) are a class of compounds that utilize the specificity of antibody-antigen interaction to achieve targeted delivery of small molecule payloads. Their high selectivity has allowed the use of potent cytotoxins as the payload to kill cancer cells. Compounds such as tubulin inhibitors, topoisomerase inhibitors, and DNA minor groove alkylators have been used as ADC payloads (Anderl et al., 2013; Polakis, 2016). Towards this direction, duocarmycins were made and experiments were carried out to

DMD Fast Forward. Published on March 11, 2019 as DOI: 10.1124/dmd.118.085209
This article has not been copyedited and formatted. The final version may differ from this version.

understand their DNA alkylation mechanisms. In this study, several bis-chloro-seco-CBIs including compounds **4** and **5** were synthesized with the CBI dimers connected by a 3,3'-(1,4-phenylene)diacryloyl group. Additionally, these compounds carry different types of side chains with variable lengths serving as handles for the antibody linkage. The DNA alkylation by duocarmycins is not only a mechanism of pharmacological activity, but also serves as a process for cells to eliminate these compounds (Kiakos et al., 2007; Ghosh et al., 2010). Since DNA adducts haven't been systemically characterized before for bis-CBI compounds to the best of our knowledge, the DNA alkylation of bis-seco-CBIs **4** and **5** were characterized in comparison with bis-seco-CBI **3** and two mono-seco-CPI **1** and **2** (Figure 1). CPI monomers **1** and **2** are the chloro seco- forms of a synthetic duocarmycin analogue with a methyl group on the pyrrole ring and the natural compound Duocarmycin SA (Mitchell et al., 1993; Robertson et al., 2010). Bis-seco-CBI **3** with a 0.1 pM *in vitro* potency previously showed DNA cross linking activity, but bis-DNA adducts were not detected from *in vitro* DNA incubations by liquid-chromatography mass spectrometry (LC-MS) (Tercel et al., 2013). In this study, we have developed and applied a novel method to induce the depurination by an acid for this class of compounds, which revealed more information regarding the DNA adduct profile and reaction mechanisms as the acidic depurination method was capable of capturing a more representative population, sometimes a different population, of DNA adducts as they existed on DNA compared to the heat depurination method that generated artificial products.. The types of adducts were characterized and the extent and kinetics of adduct formation were measured. To examine the extent of bis-alkylation and the mechanism of alkylation by bis-seco-CBIs, di-adduct vs mono-adduct ratios were also determined. Additionally, stability of the payloads was further studied as the stability together with potency of the payloads drive the *in vivo* efficacy (Zhang et al., 2018).

DMD Fast Forward. Published on March 11, 2019 as DOI: 10.1124/dmd.118.085209
This article has not been copyedited and formatted. The final version may differ from this version.

Materials and Methods

Materials. Reagents and buffers were purchased from Sigma-Aldrich if not otherwise specified. The DNA solution was prepared by dissolving genomic calf thymus DNA in water with gentle rocking overnight to a final concentration of 1 mg/mL. Self-complimentary oligo DNA 5'-CGCCTTATAAGGCG-3' were designed having 2 adenines with 0-2 base pairs apart on the same chain or 0-4 base pairs apart from the different chains. The oligonucleotides were synthesized at Genentech. The self-complimentary oligomer was dissolved in 10 mM Tris-HCl buffer to a final concentration of 1 mM; the solution was heated to 90 °C for 5 min for annealing and then cooled down to room temperature before use. Compounds **1**-**5** (Figure 1) were synthesized at Genentech with a purity >95% and detailed synthesis will be published elsewhere.

Sample processing. Compounds were initially dissolved in DMSO as stock solutions at 10 mM. Compounds (10 μM) were incubated in 10 mM Tris-HCl buffer (pH 7.4) alone for stability study or in the presence of 0.5 mg/mL calf thymus DNA or 100 μM Oligodeoxyribonucleotide for DNA alkylation study. In the kinetics study, equal volumes of the same sample were aliquoted at different time points after vortex mixing and were immediately stored in -80 °C freezer until analysis. Prior to LC-MS analysis, samples were diluted and processed for depurination as follows: 4 times dilution with water as the control group, 4 times dilution with 0.1% formic acid as the acid hydrolysis group, or 4 times dilution with water and heated at 90 °C for 10 min as the neutral thermal hydrolysis group. DNA precipitation was also conducted for comparison in which incubation mixture was mixed with three volumes of acetonitrile and centrifuged at 15,000 x g for 15 min. The supernatant was removed, and another three volumes of acetonitrile was added to wash away the residual free compounds and centrifuged to remove acetonitrile. The DNA pellet was then resuspended in 10 mM Tris-HCl buffer (pH 7.4) and processed for depurination as described above.

UHPLC-UV Mass Spectrometry Analysis. The incubation samples were analyzed by UHPLC-UV-MS/MS using Dionex Ultimate 3000 LC Systems coupled with Thermo Q Exactive Plus mass spectrometer operated in positive electrospray ionization (ESI) mode. For UHPLC-UV-MS analysis, the capillary temperature was set at 265 °C, the source potential was 3500 V and the source heater was set at 425 °C. The mass spectrometer was operated in the data-dependent scanning mode to MS^2 with dynamic exclusion enabled. The

normalized collision energy for the data-dependent scan was 30. Other potentials were adjusted to get the optimal ionization and fragmentation of the parent compounds. UV absorption spectra were obtained with the in-line diode array detector. A Thermal Hypersil GOLD C18 column (100 mm x 2.1 mm, 1.9 µm) or a Luna Omega C18 100 Å column was used (100 mm x 2.1 mm, 1.6 µm) and the compounds were eluted by a gradient of mobile phase A (0.1% formic acid in water or 20 mM ammonium acetate in water, pH 8.0) and mobile phase B (acetonitrile) (5% B 0-2 minutes, 5-20% B 2-3 minutes, 20-75% B 3-13 minutes, 75-95% B 13-15 minutes, 95% B 15-17 minutes, 95-5% B 17-17.2 minutes, and 5% B 17.2-20 minutes) at a flow rate of 0.4 mL/min at 35 °C. Relative quantities of compound –related components were estimated by mass response or UV peaks.

Cell Killing Assay. Cells were seeded in a 384-well plate (for BJAB, seeded at 10,000 cells/well) where 54 µL of DMEM/F-12 cell culture medium was supplemented with 10% FBS in each well, and after 24 hours, they were treated with compounds **1**-**5** (1:3 serial dilution with last one as medium control, quadruplicate for each concentration). Cells were incubated in a humidified incubator set at 37 °C and an atmosphere of 5% CO_2. After 4 days of drug incubation, the cell viability was determined using Promega CellTiter-Glo luminescent reagent, which measures ATP level (an indirect measure of cell number). The luminescent intensity was measured on PerkinElmer Envision reader. The relative cell viability was calculated by normalizing to non-drug treatment control and was graphed using KaleidaGraph software package. The IC_{50} value was determined as the concentration to obtain 50% of the maximum cell killing and shown in Table 1.

Results

Acidic depurination. During the initial work of DNA incubation with bis-seco-CBIs, DNA adducts were unexpectedly detected in the incubation mixture by LC-MS/MS using an acidic mobile phase without a prior depurination step. To test if these adducts were formed due to an unknown spontaneous depurination process, the samples were mixed with ethyl acetate (EA). The organic portion and aqueous portion were subsequently separated and analyzed via LC-MS/MS. However, the results showed that DNA adducts were barely detectable in the organic portion, while the aqueous portion still showed abundant DNA adduct peaks (Supplemental Figure S1). This observation ruled out a spontaneous depurination and indicated that the depurination occurred after samples were injected into the LC. It was later determined that the acidic condition of the mobile phase led to a rapid on-column depurination. When the aqueous mobile phase A was switched from 0.1% formic acid to ammonium acetate buffer at pH 8, the DNA adducts were no longer captured (Supplemental Figure S2). Consequently, the basic LC condition was used throughout the rest of the study. The novel acidic depurination method was thus applied to this study from this knowledge by adding 4 volumes of 0.1% formic acid post adduct-formation step in comparison with the traditional neutral thermal hydrolysis (heat) depurination treatment.

Reaction profile and DNA adduct identification. The chloro seco-CPI/CBI compounds were incubated with genomic DNA at 37°C for 48 hr. The samples were then split into three portions and processed with: 1) no treatment, 2) acidic depurination, or 3) heat depurination. The characterizations of depurination and degradation products are listed in Table S1. For seco-CPI monomer **1**, the UV chromatograms of acidic and heat depurination samples indicated the formation of a major UV peak at 7.86 min (**1b**) as compared to the no treatment control (Supplemental Figure S3a). Extracted ion chromatogram (XIC) of the proposed adenine adduct **1b** confirmed the corresponding peak at 7.90 min with a 0.04 min in-line delay from the UV detector. Its fragmentation pattern also matched with that of the parent compound with an additional ion of 136.0612 corresponding to the adenine fragment (Table S1). Smaller peaks at the same retention time from XIC of spirocyclized **1a** and amide hydrolysis product **1c** were likely resulted from in-source fragmentation of **1b**. Neither the parent compound **1** nor the cyclopropyl form **1a** was detected after the incubation, indicating a

DMD Fast Forward. Published on March 11, 2019 as DOI: 10.1124/dmd.118.085209
This article has not been copyedited and formatted. The final version may differ from this version.

complete reaction. Scrutinization of the MS data also found trace levels of amide hydrolysis product **1c**, which did not show up as intense peaks in the UV chromatograms.

CPI monomer **2** had comparable results with **1** (Supplemental Figure S3b). One major peak at 7.90 min (**2b**) was observed with both the acidic and heat depurination samples and identified to be the adenine adduct of **2** by both exact mass and fragmentation patterns. Small amounts of compound **2** were still detectable in the control and acidic depurination samples, but not in the heat depurination sample (small peak at 11.00 min). The cyclopropyl form (**2a**) was detected in the heat depurination sample, probably from conversion of the residual parent compound **2** and reverse alkylation from adenine adduct **2b** under heating condition. The amide hydrolysis products **2c** and **2d** were also detected in these samples.

CBI dimers were expected to have a much more complex profile due to potential mixed fates of the two CBI units. Compound **3** is a bis-seco-CBI having a 3-carbon chain in between. Unlike CPI monomers **1** and **2**, compound **3** was still the major form present after the incubation, indicating a less extensive alkylation (Supplemental Figure S3c). The spirocyclization products **3a** and **3b** occurred under the no treatment condition. Two new major UV peaks at 8.20 min and 8.58 min and a small peak at 10.22 min were observed in the acidic depurination sample, corresponding to the di-adenine adduct **3f**, hydroxyl mono-adenine adduct **3e**, and chloro mono-adenine adduct **3c**. Cyclopropyl mono-adenine adduct **3d** was detected as a minor adduct. Amide hydrolysis products **3g** and **3h** were also observed, and **3g** corresponded to the UV peak at 6.12 min. However, the heat depurination sample exhibited a quite different profile. The UV chromatogram of heat depurination sample showed general less abundant depurinated DNA adducts. Specifically, the abundant di-adenine adduct **3f** and the chloro mono-adenine adduct **3c** captured in the acidic depurination sample were not captured after heat depurination. On the other hand, abundant cyclopropyl **3b** and cyclopropyl mono-adenine adduct **3d** with equal or higher signal were observed.

For compound **4**, UV chromatograms indicated no apparent differences qualitatively between the samples processed with acidic or heat depurination with major peaks corresponding to the parent compound **4** (13.68 min), mono-spirocyclization product **4a** and **4b** (a doublet at 12.50 min and 12.61 min), and di-cyclopropyl **4c** (11.19 min) (Supplemental Figure S3d). Accordingly, small peaks of chloro mono-adenine

adduct **4d**/**4e** (single peak) with acidic depurination and cyclopropyl mono-adenine adducts **4f**/**4g** by heat depurination were detected. Di-adenine adduct **4h** was detected with much lower signal than the mono adenine adducts. Amide hydrolysis product **3g** was also captured similar to compound **3**.

Compound **5** had a more extended side chain than **4**. From the UV chromatograms, parent compound **5** (11.88 min), mono-spirocyclization product **5a** and **5b** (10.47 and 10.62 min), and di-cyclopropyl **5c** (9.13 min) were present after the incubation (Supplemental Figure S3e). The acid treated sample had a large peak at 9.70 min with several other minor peaks; while the heat treated sample showed relatively smaller peaks and was absent of the peak at 9.70 min. Fragmentation and XIC chromatograms indicated the major adduct in the acidic depurination sample being chloro mono-adenine adduct **5d**/**5e** corresponding to the peak at 9.70 min. Both depurination methods detected di-adenine adduct **5j** in smaller quantities, but cyclopropyl mono-adenine adducts **5f** and **5g** were only detected with heat depurination. Similarly, amide hydrolysis product **3g** was also captured.

Chloro mono-adenine adducts 3c, 4d/e, 5d/e found as major products under the acidic condition were not detected under heating condition. The cyclopropyl adducts 3d, 4f/g, 5f/g detected under the heating condition instead were likely artificially converted from those respective chloro mono-adenine adducts 3c, 4d/e, 5d/e that were originally exited on DNA under the heating condition.

DNA adduct formation kinetics and di to mono-adduct ratios. Compound **5** was selected to study the kinetics of DNA adduct formation. From incubation with genomic DNA, time dependent increases of the four DNA adducts, chloro mono-adenine adducts **5d**/**5e**, hydroxyl mono-adenine adducts **5h/5i**, cyclopropyl mono-adenine adducts **5f/5g**, and di-adenine adduct **5j**, were observed with chloro mono-adenine adducts **5d**/**5e** being the major adducts after acidic hydrolysis (Figure 2 & Table 2). The DNA adducts were formed in a time-dependent manner in the first 24 h of incubation. However, when the samples were processed with neutral thermal hydrolysis, di-adenine adduct **5j** represented the major adduct with cyclopropyl mono-adenine adducts **5f**/**5g** and hydroxyl mono-adenine adducts **5h/5i** being the minor adducts. By incubation of compound **5** with a designed oligomer of 14 base pairs (5'-CGCCTTATAAGGCG-3'), chloro mono-adenine adducts **5d**/**5e** was

again captured as the most abundant adduct with time-dependent formations at 37 °C, 25 °C, or 4 °C (Table 3). For the seco-CPI/CBI class of compounds, DNA alkylation could be one of the clearance pathways.

Since the bis-seco-CBI were designed to have more potent cell killing activity from intra- or interstrand cross-linking, the relative amount of di-adduct vs mono-adduct were calculated for the CBI dimers (Figure 3). For compound **5**, chloro mono-adenine adduct **5d**/**5e** and hydroxyl mono-adenine adduct **5h/5i** were the major mono-adducts determined and **5j** being the only di-adduct, thus **5j** to **5d**/**5e** + **5h/5i** ratio was determined based on UV signals. Similar to compound **5**, the most abundant adducts from compounds **3** or **4** were used for the calculation. After the incubation, the di- to mono-adduct ratios for compounds **3**, **4**, and **5** were 0.71, 0.67, and 0.08, respectively. This result demonstrated significantly different DNA adduct profiles of these CBI dimers, while all of them had dominating mono-alkylation. The higher di- to mono-adduct ratios for compounds **3** and **4** than **5** is consistent with their cell-killing potential with **5** be less potent (Table 1).

Payload stability and degradation. Degradation of the CPI monomers in buffer mainly happens with the spirocyclization resulting in the cyclopropyl form being the major form after 24 h of incubation for both CPI-monomers (Figure 4a & 4b). The cyclopropyl forms correspond to the largest peaks at 9.61 min for compound **1** and 9.68 min for compound **2**. Since the cyclopropyl forms of the compounds still contain the same designed activity, this particular degradant should not affect the effectiveness of the payload. Amide hydrolysis represents another major degradation pathway for these chloro seco-CPI/CBI compounds with the detection of **2c** and **2d**. Additionally, solvolysis product **2e** was observed in relatively low quantities, similar to what was previously reported (Boger and Garbaccio, 1999a).

Comparatively, incubation of compound **3** in buffer showed two small peaks in the UV chromatogram corresponding to di-cyclopropyl **3b** and amide hydrolysis product **3g** (Figure 4c). Compound **4** was more stable than compound **3**, with compound **4**, mono-cyclopropyl **4a** and **4b**, and di-cyclopropyl **4c** present in the UV chromatogram and **3g** only detected by mass spec (Figure 4d). Incubation of compound **5** in buffer also resulted detection of compound **5** and mono- and di- spirocyclization products **5a**, **5b**, and **5c**, with di-cyclopropyl **5c** being the major peak (Figure 4e). High levels of amide hydrolysis products **3g** and **5k**/**5l** were also detected. Compound **5** showed more rapid degradation at higher temperatures as expected with 2.5%,

10%, and 20% parent remaining after incubation in buffer at 37 °C, 25 °C, or 4 °C for 48 hr (Table 4, Supplemental Figure S4). In the presence of DNA, however, stability of the compounds was significantly increased. In comparison, around 25% of compound **5** was still present after 24 h at 37 °C with the presence of genomic DNA (Figure S3). When DNA precipitation was performed after the incubation, a colored DNA precipitate (yellowish color from the compounds) was observed.

To bridge the differences between the two depurination methods and to further verify the chloro mono-adenine adducts, the DNA incubation sample from compound **5** was aliquoted and heated at 25 °C, 55 °C, 75 °C, or 90 °C respectively. Excitingly, significant amount of chloro mono-adenine adduct **5d**/**5e** was captured after heating at 55 °C, further verifying the existence of this chloro adduct (Supplemental Figure S5). As the temperature increased, the amount of **5d**/**5e** decreased, which likely led to conversion to the cyclopropyl adduct forms. The increasing amount of di-adenine adduct **5j** formation from 75 °C to 90 °C, the temperature used in the original heat depurination method, may suggest that a higher energy was required to release di-alkylated DNA adducts. However, the heating condition would also led to artificial reactions including reverse dealkylation and spirocyclization. Thus, the acidic depurination could minimize reverse dealkylation and showed cleaner results from less artificial reactions with both adducts detected. Nonetheless, an enzymatic digestion method can be used to further compare the efficiencies of the chemical depurination and potential associated side reactions.

DMD Fast Forward. Published on March 11, 2019 as DOI: 10.1124/dmd.118.085209
This article has not been copyedited and formatted. The final version may differ from this version.

Discussion

Significance of studying DNA alkylation

Duocarmycins exert cytotoxicity through DNA minor groove binding and alkylation, interfering with transcriptional activities and causing DNA damage (Kiakos et al., 2007; Ghosh et al., 2010). Bis-CPI/CBIs are potential drug candidates because of their enhanced cytotoxicity from DNA cross-linking, but are difficult to be analyzed for structure-activity correlation because of their DNA reactivity. In addition, the DNA alkylation could be a mechanism for the clearance of the compounds from circulation then the bound drug can be eliminated through DNA nucleotide excision repair or degradation of DNA of lysed cells. (Kiakos et al., 2007). The DNA bound alkylators could otherwise stay and accumulate in cells (Ma et al., 2016). Thus, DNA alkylation serves both as a mechanistic process for cell killing and a clearance pathway for the duocarmycins. Understanding the DNA alkylation properties of these compounds could help better correlate *in vivo* efficacy and off-target toxicity.

Depurination method to study mono- and di-DNA alkylation

DNA adduct characterization normally requires the release of adducts from DNA, i.e. depurination. Neutral thermal hydrolysis has been extensively used previously for CPI/CBI DNA alkylation studies (Lee and Gibson, 1993; Boger and Johnson, 1996; Tercel et al., 2013). However, unwanted reverse alkylation reactions and amide hydrolysis have been reported especially under elevated temperatures (Warpehoski et al., 1992; Lee and Gibson, 1993; Asai et al., 1994; Elgersma et al., 2015). Acidic hydrolysis depurination has been reported (Leung et al., 2016), but not applied to CPI/CBI studies previously. In this study, the acidic hydrolysis exhibited rapid and effective depurination for CPI/CBI DNA adducts (Supplemental Figure S6), which could be attributed to a destabilized glycosidic bond from protonation of adenines (Scheme 2). Additionally, the acidic depurination process was also milder than neutral thermal hydrolysis with more abundant adducts that originally existed on DNA detected in general and the detection of novel chloro mono-adenine adducts from chloro seco-CBI dimers.

DMD Fast Forward. Published on March 11, 2019 as DOI: 10.1124/dmd.118.085209
This article has not been copyedited and formatted. The final version may differ from this version.

Particularly, compound **3** was previously determined to cause extensive DNA cross-linking using agarose gel electrophoresis. (Tercel et al., 2013). However, only cyclopropyl mono-adenine adduct (**3d**) was detected with LC-MS analysis. In this study, a similar result was obtained after neutral thermal hydrolysis with **3d** being the only DNA adduct detected. However, the acidic hydrolysis captured additional and abundant di-adenine adduct **3f**, which supported its DNA cross-linking activity (Supplemental Figure S3c). The cyclopropyl mono-adenine adduct **3d** observed from neutral thermal hydrolysis was likely form through spirocyclization of chloro mono-adenine adduct **3c** that existed on DNA. Reverse alkylation of di-adenine adduct **3f** to form **3d** is also possible under the heating condition. . Similarly for compounds **4** and **5**, much higher levels of chloro mono-adenine adducts were observed after acidic depurination but not with heat depurination. Under the heating condition, these chloro mono-adenine adducts were artificially converted to the cyclopropyl forms. From this study, the DNA adduct profiles also reiterated the selective adenine alkylation nature of these seco-CPI/CBI compounds. Although detectable guanine adducts were previously reported (Mitchell et al., 1993), they were not observed in this study.

A previous study of bizelesin estimated a potential di- to mono-alkylation ratio (DMR) around 0.5 from thermal DNA strand breakage assay (Sun and Hurley, 1993). When assessing the extent of di-alkylation in this study, compound **3** and **4** showed slightly higher DMR around 0.7, whereas compound **5** had much higher level of mono adducts over di adducts, with a DMR less than 0.1 (Figure 5). The data indicated the long side chain on the linker between CBI units in compound **5** might hamper the secondary alkylation, thus making the mono-adduct being a much more dominant form. The lower extent of di-alkylation with compound **5** also correlated with a >20-fold lower *in vitro* activity compared to compounds **3** and **4** (Table 1). The similar IC_{50} values of compounds **3** and **4** and much higher IC_{50} of compound **5** were also somewhat in line with a previous finding that smaller and more hydrophobic duocarmycins exerted more potent cytotoxicity (Wolfe et al., 2013).

Mechanism of DNA alkylation

It's commonly accepted that spirocyclization of seco-CBI/CPI precedes its DNA alkylation with the cyclopropane CBI/CPIs being the active forms (Jia and Lown, 2000; Kupchinsky et al., 2004; Elgersma et al., 2015). However, the results of bis-seco-CBIs from this study also supported the potential of DNA alkylation

without prior spirocyclization. The observation of chloro mono-adenine adduct **5d**/**5e** as the dominant adduct form for compound **5** and much lower levels of cyclopropyl mono-adenine adduct **5f**/**5g** suggested that the chloro seco-CBI/CPIs potentially reacted with adenine without prior spirocyclization. It's hypothesized to form an electrophilic chloro cyclopropyl intermediate, which further alkylate DNA via a similar S_N2 mechanism (Scheme 1). In support of this hypothesis, previous studies from the Boger lab reported the DNA alkylation and cell killing activities of synthetic mono seco-CPIs that cannot spirocyclize due to replacement of the hydroxyl group on the alkylation indole with a methoxy group or a hydrogen (Boger et al., 1990; Jin et al., 2007).

Another interesting observation was that although two stereoisomers were observed from spirocyclization of compounds **4** and **5**, only single peaks were captured for mono-adenine adducts (Figure S3d and S3e). One exception was the doublet peaks in the XIC chromatogram of cyclopropyl mono-adenine adduct **5f**/**5g** from neutral thermal hydrolysis, which possibly resulted from spirocyclization of chloro mono-adenine adduct **5d**/**5e** and reverse alkylation of di-adenine adduct **5j**. This result supported a specific DNA binding conformation with one alkylation side much more reactive than the other and the sequential di-alkylation happening in a specific order. The DNA alkylation results from DNA and the designed oligodeoxyribonucleotide incubations were also consistent qualitatively, indicating the di-alkylation happened within 4 base pairs apart (Table 3).

Payload stability/degradation and DNA alkylation activity

Stability/degradation of these compounds under physiological condition is also important for their *in vivo* efficacy (Zhang et al., 2018). Boger et al. have previously shown a hyperbolic correlation between stability and DNA alkylation of CPI/CBIs, which a fine balance between stability and reactivity enables the availability of CPI/CBI to reach DNA minor groove and alkylation of DNA through a twist induced activation (MacMillan and Boger, 2009). After 24 h incubation in Tris-HCl buffer at pH 7.4, most of the test compounds were spirocyclized to the cyclopropyl forms (Figure 4), but still contain DNA alkylation activity. Time dependent analysis of compound **5** showed that it had half-lives of 21 min, 47 min, and 170 min at 37 °C, 25 °C, and 4 °C, respectively in forming spirocyclized products (Table 4 & Supplemental Figure S4). In comparison, bizelesin

was reported to have a longer half-life of 2.1 h at pH 7 in buffer in forming mono- and di-cyclized products (Walker et al., 1994).

Consistent with previous reports, the major degradation pathway observed was the amide hydrolysis with the release of CBI/CPI alkylating groups and loss of DNA alkylation activity (Elgersma et al., 2015). The released alkylating groups have shown >50,000-fold less activity, and thus can also be considered as a clearance transformation pathway. The amide hydrolysis seemed to be common in these compounds. The terminal amine on the side chain of **5** potentially facilitated the hydrolysis by attacking the amide bond, resulting in compound **5** having much more hydrolysis than **4** (Figure 4d & 4e). Elgersma et al. also discussed the amide hydrolysis only happened after spirocyclization due to the vinylogous amide bond formed, which was consistent with the result from this study. Compound **3** and **5** had much higher released alkylating group **3g** with almost complete spirocyclization after 24 hours, while **4** showed much less spirocyclization and amide hydrolysis. Nevertheless, in the presence of DNA, much less degradation was observed, which was probably due to a protective effect of the DNA minor groove (Supplemental Figure S3). Small fractions of chloro seco parent compounds were even detected in the DNA precipitate after being extracted with ethyl acetate, indicating the tight binding nature of these compounds on DNA.

Solvolysis of the CPI/CBI compounds can be considered as another degradation pathway and the extent in acidic buffer has been used to assess the reactivity against common nucleophiles (Tercel et al., 2014). However, CPI/CBIs have shown to be mostly inert under physicological conditions (Boger and Garbaccio, 1999a). In this study, solvolysis was minimal in buffer at pH 7.4, with only seco-CPI **2** having detectable solvolysis product **2e** (Figure 3b). Acute formic acid treatment of the samples showed increased solvolysis products of CPI **1** and **2**, but not for bis-CBI **3**, **4**, and **5**, indicating the CBIs were more stable and less prone to solvolysis related degradation as previously observed (Boger et al., 1991).

Overall, acidic hydrolysis depurination was applied to CPI/CBI studies with more rapid/thorough depurination than traditional neutral thermal hydrolysis. More importantly, the acidic depurination method was capable of capturing a more representative population, sometimes a different population with compound **3**, of DNA adducts as they existed on DNA compared to the heat depurination method in which chloro mono-

DMD Fast Forward. Published on March 11, 2019 as DOI: 10.1124/dmd.118.085209
This article has not been copyedited and formatted. The final version may differ from this version.

adenine adducts were converted to the cyclopropyl forms. As a result, the di- to mono-adduct ratios for di-alkylators is consistent with their cell-killing potential. Several novel mono- and di-adenine adducts have been characterized and the DNA alkylation activity and profile can be largely affected by the type and size of the linker of bis-seco-CBIs. Although both mono- and di- alkylation adducts have been observed, mono-adenine adducts were still the major forms. The detection of a novel chloro mono-adenine adduct as a major form also indicated a potential mechanism of direct alkylation without prior spirocyclization. In addition, the bis-seco-CBIs can rapidly undergo spirocyclization and amide hydrolysis in buffer, but exhibited much higher stability in the presence of DNA. These findings should be helpful to explain *in vitro in vivo* efficacy correlations and better design of duocarmycins as ADC payloads. The findings in this study provided an effective analytical tool to evaluate DNA alkylators and to study the DNA alkylation that is a disposition mechanism of these compounds.

Acknowledgements

We'd like to sincerely thank Marcel Hop and Andy Polson for valuable discussions in the project. We'd also like to thank Peter Ng for help in synthesizing and providing the Oligomers.

Authorship contributions:

Study designs: S Wang, Philips, Khojasteh, D Zhang

Reagents amd methods: S Wang, Pillow, Dragovich, Staben, Ma, Su, J Wang, Sangaraju

Experimentals: S Wang, C Zhang, Bobba, Sangaraju, Guo

Data analysis: S Wang, Chen, C Zhang, Bobba, J Wang, Sangaraju, Wei, Lewis Philips, Khojasteh, D Zhang

Writing the manuscript: S Wang, Chen, J Wang, Sangaraju, Khojasteh, D Zhang

References

Anderl J, Faulstich H, Hechler T, and Kulke M (2013) Antibody–Drug Conjugate Payloads, in: *Antibody-Drug Conjugates* (Ducry L ed), pp 51-70, Humana Press, Totowa, NJ.

Asai A, Nagamura S, Saito H, Takahashi I, and Nakano H (1994) The reversible DNA-alkylating activity of duocarmycin and its analogues. *Nucleic Acids Research* **22:**88-93.

Baraldi PG, Bovero A, Fruttarolo F, Preti D, Tabrizi MA, Pavani MG, and Romagnoli R (2004) DNA minor groove binders as potential antitumor and antimicrobial agents. *Med Res Rev* **24:**475-528.

Boger DL and Garbaccio RM (1999a) Are the duocarmycin and CC-1065 DNA alkylation reactions acid-catalyzed? Solvolysis pH-rate profiles suggest they are not. *J Org Chem* **64:**5666-5669.

Boger DL and Garbaccio RM (1999b) A Novel Class of CC-1065 and Duocarmycin Analogues Subject to Mitomycin-Related Reductive Activation. *The Journal of Organic Chemistry* **64:**8350-8362.

Boger DL, Ishizaki T, Zarrinmayeh H, Munk SA, Kitos PA, and Suntornwat O (1990) Duocarmycin-pyrindamycin DNA alkylation properties and identification, synthesis, and evaluation of agents incorporating the pharmacophore of the duocarmycin-pyrindamycin alkylation subunit. Identification of the CC-1065 duocarmycin common pharmacophore. *Journal of the American Chemical Society* **112:**8961-8971.

Boger DL and Johnson DS (1995) CC-1065 and the duocarmycins: unraveling the keys to a new class of naturally derived DNA alkylating agents. *Proceedings of the National Academy of Sciences* **92:**3642-3649.

Boger DL and Johnson DS (1996) CC-1065 and the Duocarmycins: Understanding their Biological Function through Mechanistic Studies. *Angewandte Chemie International Edition in English* **35:**1438-1474.

Boger DL, Munk SA, and Ishizaki T (1991) (+)-CC-1065 DNA alkylation: observation of an unexpected relationship between cyclopropane electrophile reactivity and the intensity of DNA alkylation. *Journal of the American Chemical Society* **113:**2779-2780.

Boger DL, Searcey M, Tse WC, and Jin Q (2000) Bifunctional alkylating agents derived from duocarmycin SA: potent antitumor activity with altered sequence selectivity. *Bioorganic & Medicinal Chemistry Letters* **10:**495-498.

Elgersma RC, Coumans RGE, Huijbregts T, Menge WMPB, Joosten JAF, Spijker HJ, de Groot FMH, van der Lee MMC, Ubink R, van den Dobbelsteen DJ, Egging DF, Dokter WHA, Verheijden GFM, Lemmens JM, Timmers CM, and Beusker PH (2015) Design, Synthesis, and Evaluation of Linker-Duocarmycin Payloads: Toward Selection of HER2-Targeting Antibody–Drug Conjugate SYD985. *Molecular Pharmaceutics* **12:**1813-1835.

Fukuda Y, Seto S, Furuta H, Ebisu H, Oomori Y, and Terashima S (1998) The novel cyclopropapyrroloindole (CPI) bisalkylators bearing 3,3'-(1,4-phenylene)diacryloyl group as a linker. *Bioorganic & Medicinal Chemistry Letters* **8:**2003-2004.

Ghosh S, Majumder P, Pradhan SK, and Dasgupta D (2010) Mechanism of interaction of small transcription inhibitors with DNA in the context of chromatin and telomere. *Biochimica et Biophysica Acta (BBA) - Gene Regulatory Mechanisms* **1799:**795-809.

Jia G and Lown JW (2000) Design, synthesis and cytotoxicity evaluation of 1-chloromethyl-5-hydroxy-1,2-dihydro-3H-benz[e]indole (seco-CBI) dimers. *Bioorganic & medicinal chemistry* **8:**1607-1617.

Jin W, Trzupek JD, Rayl TJ, Broward MA, Vielhauer GA, Weir SJ, Hwang I, and Boger DL (2007) A Unique Class of Duocarmycin and CC-1065 Analogues Subject to Reductive Activation. *Journal of the American Chemical Society* **129:**15391-15397.

Kiakos K, Sato A, Asao T, McHugh PJ, Lee M, and Hartley JA (2007) DNA sequence–selective adenine alkylation, mechanism of adduct repair, and in vivo antitumor activity of the novel achiral seco-amino-cyclopropylbenz[e]indolone analogue of duocarmycin AS-I-145. *Molecular Cancer Therapeutics* **6:**2708-2718.

Kupchinsky S, Centioni S, Howard T, Trzupek J, Roller S, Carnahan V, Townes H, Purnell B, Price C, Handl H, Summerville K, Johnson K, Toth J, Hudson S, Kiakos K, Hartley JA, and Lee M (2004) A novel class of achiral seco-analogs of CC-1065 and the duocarmycins: design, synthesis, DNA binding, and anticancer properties. *Bioorganic & medicinal chemistry* **12:**6221-6236.

Lee C-S and Gibson NW (1993) DNA interstrand cross-links induced by the cyclopropylpyrroloindole antitumor agent bizelesin are reversible upon exposure to alkali. *Biochemistry* **32:**9108-9114.

Leung EMK, Deng K, Wong T-Y, and Chan W (2016) Determination of DNA adducts by combining acid-catalyzed hydrolysis and chromatographic analysis of the carcinogen-modified nucleobases. *Analytical and Bioanalytical Chemistry* **408:**953-961.

Ma Y, Khojasteh SC, Hop C, Erickson HK, Polson A, Pillow TH, Yu SF, Wang H, Dragovich PS, and Zhang DL (2016) Antibody Drug Conjugates Differentiate Uptake and DNA Alkylation of Pyrrolobenzodiazepines in Tumors from Organs of Xenograft Mice. *Drug Metab Dispos* **44:**1958-1962.

MacMillan KS and Boger DL (2009) Fundamental Relationships between Structure, Reactivity, and Biological Activity for the Duocarmycins and CC-1065. *Journal of Medicinal Chemistry* **52:**5771-5780.

McGovren JP, Clarke GL, Pratt EA, and DeKoning TF (1984) Preliminary toxicity studies with the DNA-binding antibiotic, CC-1065. *The Journal of antibiotics* **37:**63-70.

Mitchell MA, Johnson PD, Williams MG, and Aristoff PA (1989) Interstrand DNA cross-linking with dimers of the spirocyclopropyl alkylating moiety of CC-1065. *Journal of the American Chemical Society* **111:**6428-6429.

Mitchell MA, Weiland KL, Aristoff PA, Johnson PD, and Dooley TP (1993) Sequence-selective guanine reactivity by Duocarmycin-A. *Chem Res Toxicol* **6:**421-424.

Polakis P (2016) Antibody Drug Conjugates for Cancer Therapy. *Pharmacological Reviews* **68:**3-19.

Robertson WM, Kastrinsky DB, Hwang I, and Boger DL (2010) Synthesis and evaluation of a series of C5'-substituted duocarmycin SA analogs. *Bioorganic & Medicinal Chemistry Letters* **20:**2722-2725.

Schwartz GH, Patnaik A, Hammond LA, Rizzo J, Berg K, Von Hoff DD, and Rowinsky EK (2003) A phase I study of bizelesin, a highly potent and selective DNA-interactive agent, in patients with advanced solid malignancies. *Annals of Oncology* **14:**775-782.

Sun D and Hurley LH (1993) Analysis of the monoalkylation and cross-linking sequence specificity of bizelesin, a bifunctional alkylation agent related to (+)-CC-1065. *Journal of the American Chemical Society* **115:**5925-5933.

Tercel M, McManaway SP, Leung E, Liyanage HDS, Lu G-L, and Pruijn FB (2013) The Cytotoxicity of Duocarmycin Analogues is Mediated through Alkylation of DNA, not Aldehyde Dehydrogenase 1: A Comment. *Angewandte Chemie International Edition* **52:**5442-5446.

Tercel M, Pruijn FB, O' Connor PD, Liyanage HDS, Atwell GJ, and Alix SM (2014) Mechanism of Action of AminoCBIs: Highly Reactive but Highly Cytotoxic Analogues of the Duocarmycins. *ChemBioChem* **15:**1998-2006.

Tichenor MS, MacMillan KS, Stover JS, Wolkenberg SE, Pavani MG, Zanella L, Zaid AN, Spalluto G, Rayl TJ, Hwang I, Baraldi PG, and Boger DL (2007) Rational Design, Synthesis, and Evaluation of Key Analogues of CC-1065 and the Duocarmycins. *Journal of the American Chemical Society* **129:**14092-14099.

Tietze LF and von Hof JM (2011) Bifunktionale Prodrugs und Drugs, Google Patents.

Walker DL, Reid JM, and Ames MM (1994) Preclinical pharmacology of bizelesin, a potent bifunctional analog of the DNA-binding antibiotic CC-1065. *Cancer Chemotherapy and Pharmacology* **34:**317-322.

Warpehoski MA, Harper DE, Mitchell MA, and Monroe TJ (1992) Reversibility of the covalent reaction of CC-1065 and analogs with DNA. *Biochemistry* **31:**2502-2508.

Wolfe AL, Duncan KK, Lajiness JP, Zhu K, Duerfeldt AS, and Boger DL (2013) A Fundamental Relationship between Hydrophobic Properties and Biological Activity for the Duocarmycin Class of DNA-Alkylating Antitumor Drugs: Hydrophobic-Binding-Driven Bonding. *Journal of Medicinal Chemistry* **56:**6845-6857.

Yasuzawa T, Muroi K, Ichimura M, Takahashi I, Ogawa T, Takahashi K, Sano H, and Saitoh Y (1995) Duocarmycins, potent antitumor antibiotics produced by Streptomyces sp. structures and chemistry. *Chemical & pharmaceutical bulletin* **43:**378-391.

Zhang DL, Le H, dela Cruz-Chuh J, Bobba S, Guo J, Staben L, Zhang CH, Ma Y, Kozak KR, Phillips GDL, Vollmar BS, Sadowsky JD, Vandlen R, Wei BQ, Su D, Fan P, Dragovich PS, Khojasteh SC, Hop C, and Pillow TH (2018) Immolation of p-Aminobenzyl Ether Linker and Payload Potency and Stability Determine the Cell-Killing Activity of Antibody-Drug Conjugates with Phenol-Containing Payloads. *Bioconjugate Chem* **29:**267-274.

DMD Fast Forward. Published on March 11, 2019 as DOI: 10.1124/dmd.118.085209
This article has not been copyedited and formatted. The final version may differ from this version.

DMD Fast Forward. Published on March 11, 2019 as DOI: 10.1124/dmd.118.085209
This article has not been copyedited and formatted. The final version may differ from this version.

Schemes

Scheme 1. Seco-CPI spirocyclization and DNA alkylation.

Scheme 2. Proposed mechanism of acidic depurination, heat depurination and reverse alkylation of CBI-adenine adducts.

Figures

Figure 1. Structures of CBI/CPI compounds used in this study. Six seco-CBI/CPI monomer or dimer compounds were used in this study: compounds **1** and **2** are seco-CPI monomers and compounds **3**, **4**, and **5** are seco-CBI dimers.

Figure 2. Kinetics of DNA adduct formation and mono-adduct/di-adduct ratios with dimer-CBI. Time dependent release of DNA adducts from compound **5** was plotted under two different depurination conditions. Ratios of major mono-adduct/di-adduct from compounds **3**, **4**, and **5** were graphed with UV peak area calculations.

Figure 3. UV semi-quantitation of mono- and di- adducts of CBI dimers. UV peak areas were quantified from the chromatograms of acidic depurination samples of **3**, **4**, and **5** DNA incubations. (Ade-Cl: mono-adenine alkylation; Ade-OH: adenine alkylation and hydroxylation; Ade-Ade: di-adenine alkylation)

Figure 4. Degradation products identified from compound incubation in buffer. CBI/CPI compounds (10 μM) were incubated in 10 mM Tris-HCl buffer (pH 7.4) at 37 °C for 24 hr before analysis. Samples were diluted 4 times with water or 0.1% formic acid in water and injected into LC-UV-MS/MS for analysis.

Tables

Table 1. *In vitro* cell killing IC_{50} values (pM) of compounds **1**-**5** in 6 different cancer cell lines after 4 days of incubation. (KPL-4 Her2 positive; SK-BR-3: Her2 overexpression; T-47D: Her2 negative; HCC1937: Her2 negative; NCI-H1781: Her2 mutant; SW 900 lung cancer cell line)

Compound	KPL-4	SK-BR-3	T-47D	HCC1937	NCI-H1781	SW 900
1	3.6	9.8	20	25	1.7	1.6
2	36	53	94	72	17	18
3	1.5	1.6	2.1	29	0.47	8.8
4	3.7	2.4	2.7	16	1.7	1.1
5	92	150	75	430	45	27

Table 2. Normalized time dependent DNA adduct profile of compound **5** and genomic DNA incubations (data normalized to compound **5** MS peak area at 0.25 h in the acidic depurination group).

Depurination	Compounds & Reactions		R.T. (min)	Relative amount of products						
				0.25 h	0.5 h	1 h	2 h	4 h	8 h	24 h
Formic acid	**5**		11.9	**1.0**	0.57	0.44	0.41	0.36	0.41	0.25
	5a/5b	mono-spirocyclization	10.5, 10.6	0.45	0.20	0.13	0.12	0.12	0.29	0.23
	5c	di-spirocyclization	9.1	0.20	0.09	0.06	0.05	0.05	0.17	0.15
	5d/5e	mono-adenine alkylation	9.7	0.14	0.27	0.28	0.41	0.47	0.65	0.88
	5f/5g	adenine alkylation and spirocyclization	8.5	0	0	0	0	0.01	0.01	0.02
	5h/5i	adenine alkylation and hydroxylation	8.3	0.01	0.03	0.03	0.05	0.06	0.08	0.15
	5j	di-adenine alkylation	8	0	0	0	0.02	0.04	0.07	0.15
Heating	**5**		11.9	0.13	0.27	0.23	0.31	0.33	0.16	0.04
	5a/5b	mono-spirocyclization	10.5, 10.6	0.09	0.51	0.27	0.57	0.81	0.07	0.01
	5c	di-spirocyclization	9.1	0.34	1.05	0.58	1.49	1.75	0.30	0.04
	5d/5e	mono-adenine alkylation	9.7	0	0	0	0.02	0.01	0.01	0
	5f/5g	adenine alkylation and spirocyclization	8.5	0.09	0.14	0.22	0.30	0.23	0.30	0.16
	5h/5i	adenine alkylation and hydroxylation	8.3	0.02	0.03	0.06	0.11	0.09	0.14	0.11
	5j	di-adenine alkylation	8	0	0.07	0.14	0.27	0.26	0.88	0.66

Table 3. Normalized time dependent formation of **5d**/**5e** and **5j** from compound **5** and Oligo incubations with acidic depurination (data normalized to **5d/5e** MS peak area at 48 h from 37 ° incubation).

Temperature	Compounds & Reactions		R.T. (min)	Relative amount of products							
				0.25 h	**0.5 h**	**1 h**	**2 h**	**4 h**	**8 h**	**24 h**	**48 h**
4 °C	**5d/5e**	mono-adenine alkylation	9.7						0.20	0.52	0.84
	5j	di-adenine alkylation	8								
25 °C	**5d/5e**	mono-adenine alkylation	9.7				0.09	0.51	1.4	2.0	2.5
	5j	di-adenine alkylation	8								
37 °C	**5d/5e**	mono-adenine alkylation	9.7		0.06	0.25	0.64	0.33	0.99	0.68	**1.0**
	5j	di-adenine alkylation	8								0.26

Table 4. Normalized degradation of compound **5** in Tris-HCl buffer (pH 7.4) at 4 °C, 25 °C, and 37 ° C (data normalized to compound **5** MS peak area at 0.25 h from 4 °C group).

Temperature	Compounds & Reactions		R.T. (min)	Relative amount of products							
				0.25 h	0.5 h	1 h	2 h	4 h	8 h	24 h	48 h
4 °C	**5**		11.9	**1.0**	0.96	0.72	0.63	0.62	0.42	0.26	0.20
	5a/5b	mono-spirocyclization	10.5, 10.6	1.4	1.9	1.3	1.4	1.1	0.95	0.71	0.56
	5c	di-spirocyclization	9.1	1.3	2.5	1.7	2.5	2.3	2.2	3.3	3.8
25 °C	**5**		11.9	0.69	0.61	0.46	0.38	0.22	0.19	0.09	0.06
	5a/5b	mono-spirocyclization	10.5, 10.6	1.3	1.2	0.96	0.81	0.51	0.48	0.27	0.20
	5c	di-spirocyclization	9.1	1.7	2.2	2.0	3.4	2.3	3.9	2.4	1.8
37 °C	**5**		11.9	0.50	0.22	0.13	0.11	0.08	0.06	0.05	0.01
	5a/5b	mono-spirocyclization	10.5, 10.6	1.1	0.52	0.35	0.28	0.23	0.20	0.19	0.07
	5c	di-spirocyclization	9.1	3.3	1.4	1.8	1.8	2.0	2.2	3.1	0.90

Figure 1.

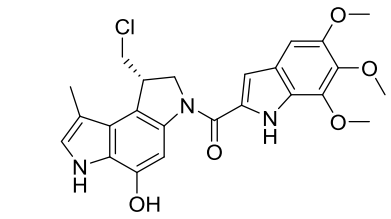

1

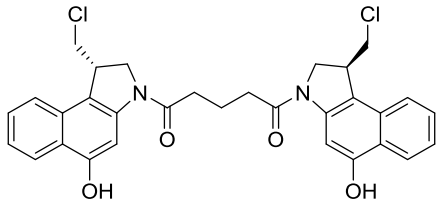

3

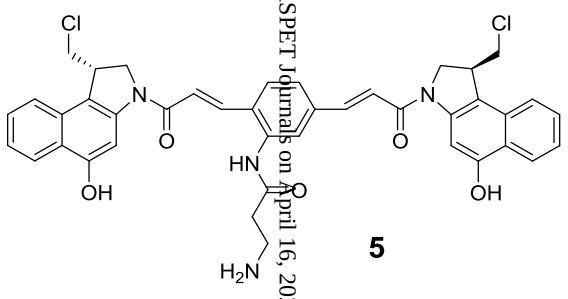

5

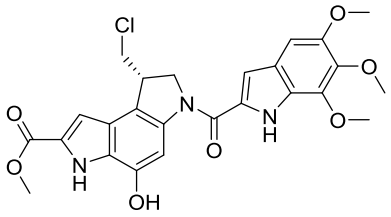

2

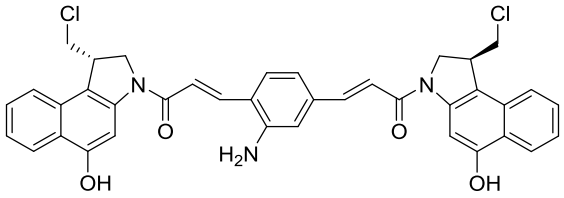

4

Figure 2.

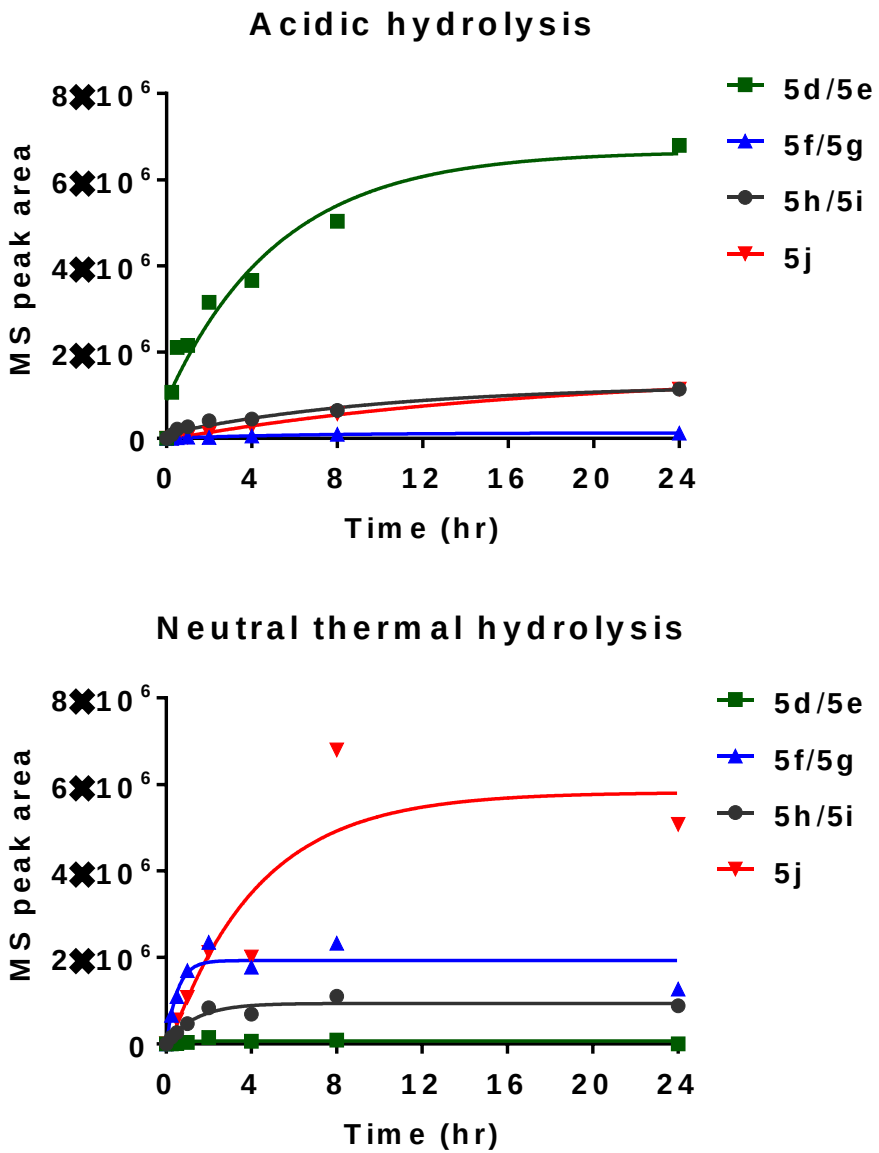

Figure 3.

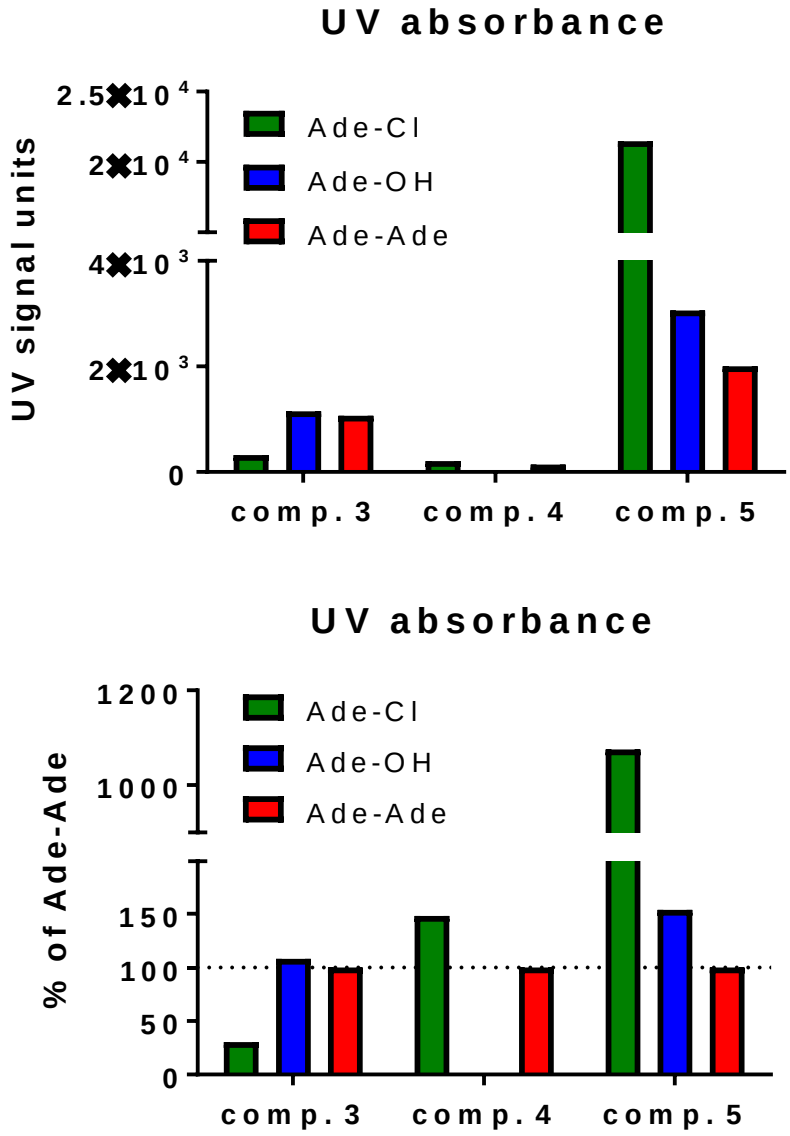

Figure 4 a, b, c

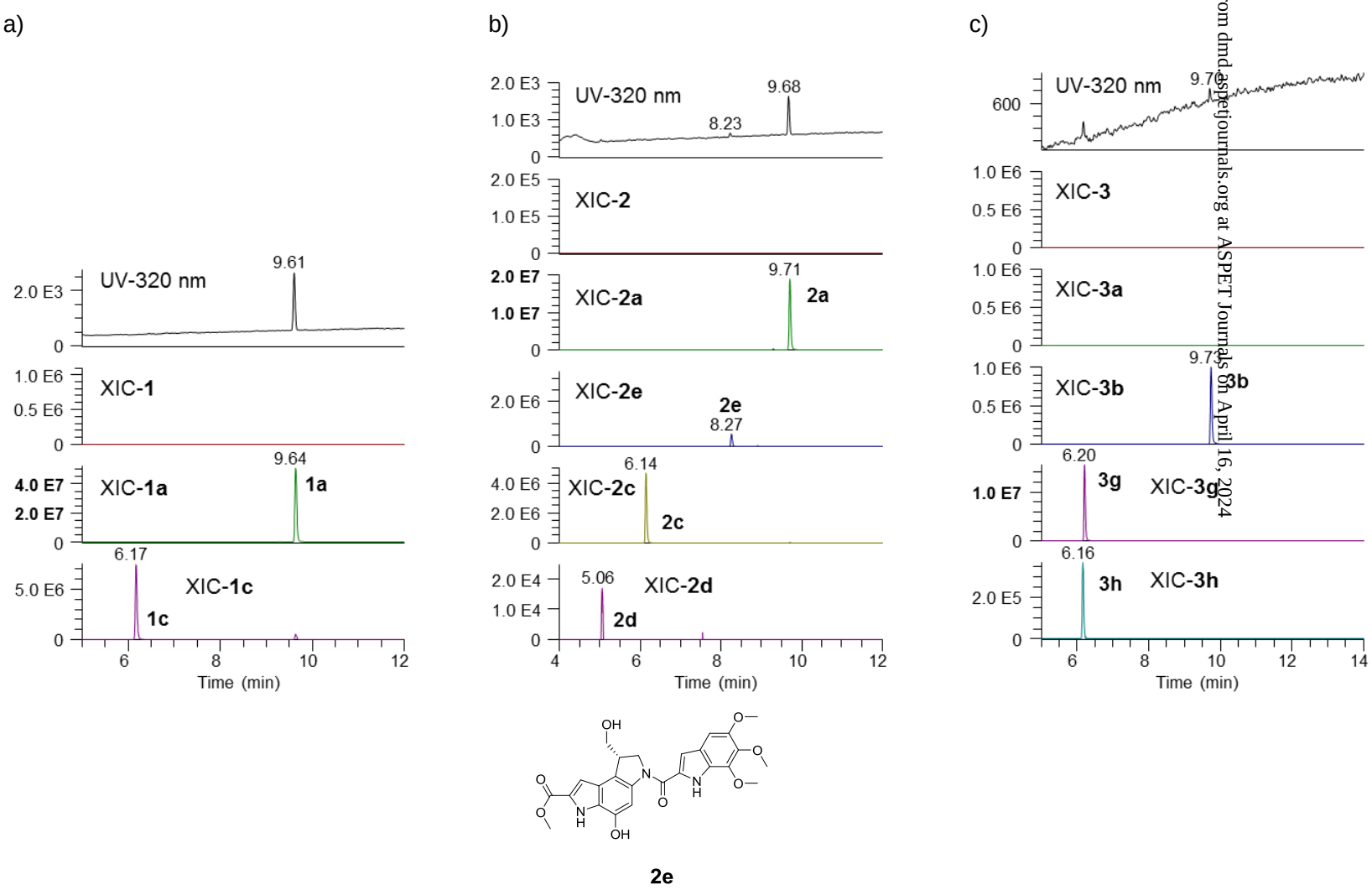

2e

Figure 4 d,e

d)

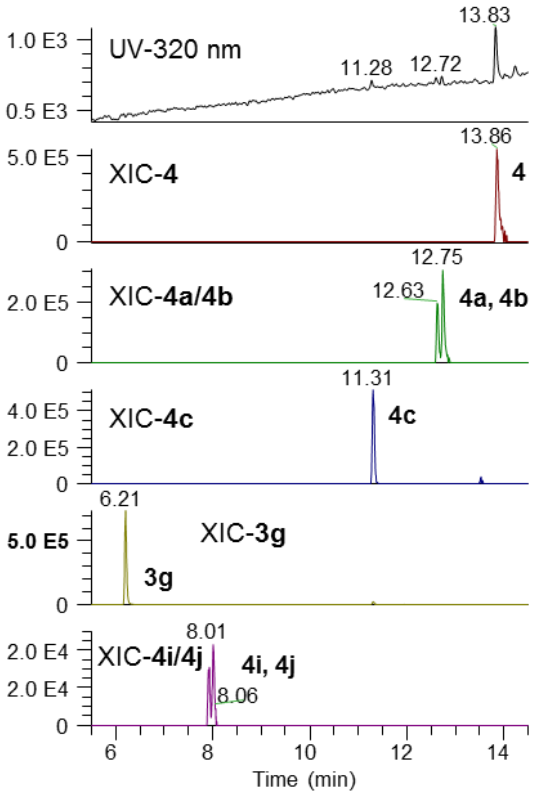

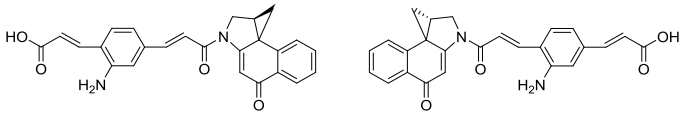

4i

4j

e)

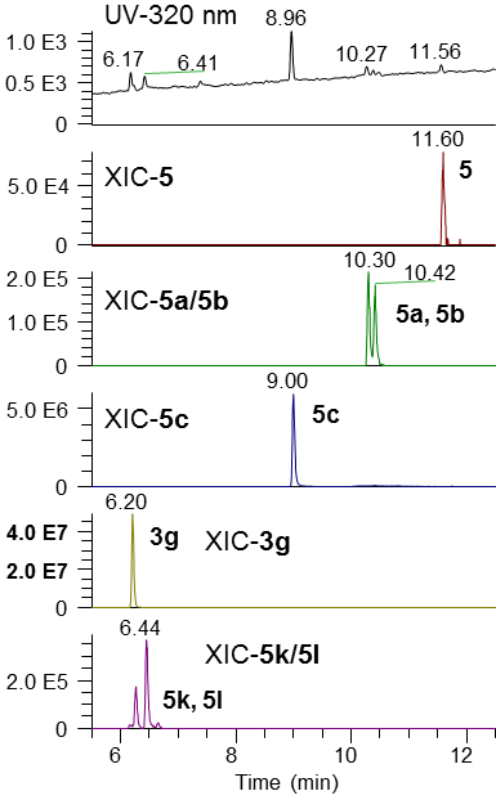

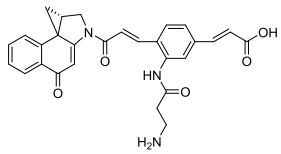

5k

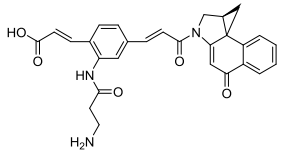

5l

Scheme 1.

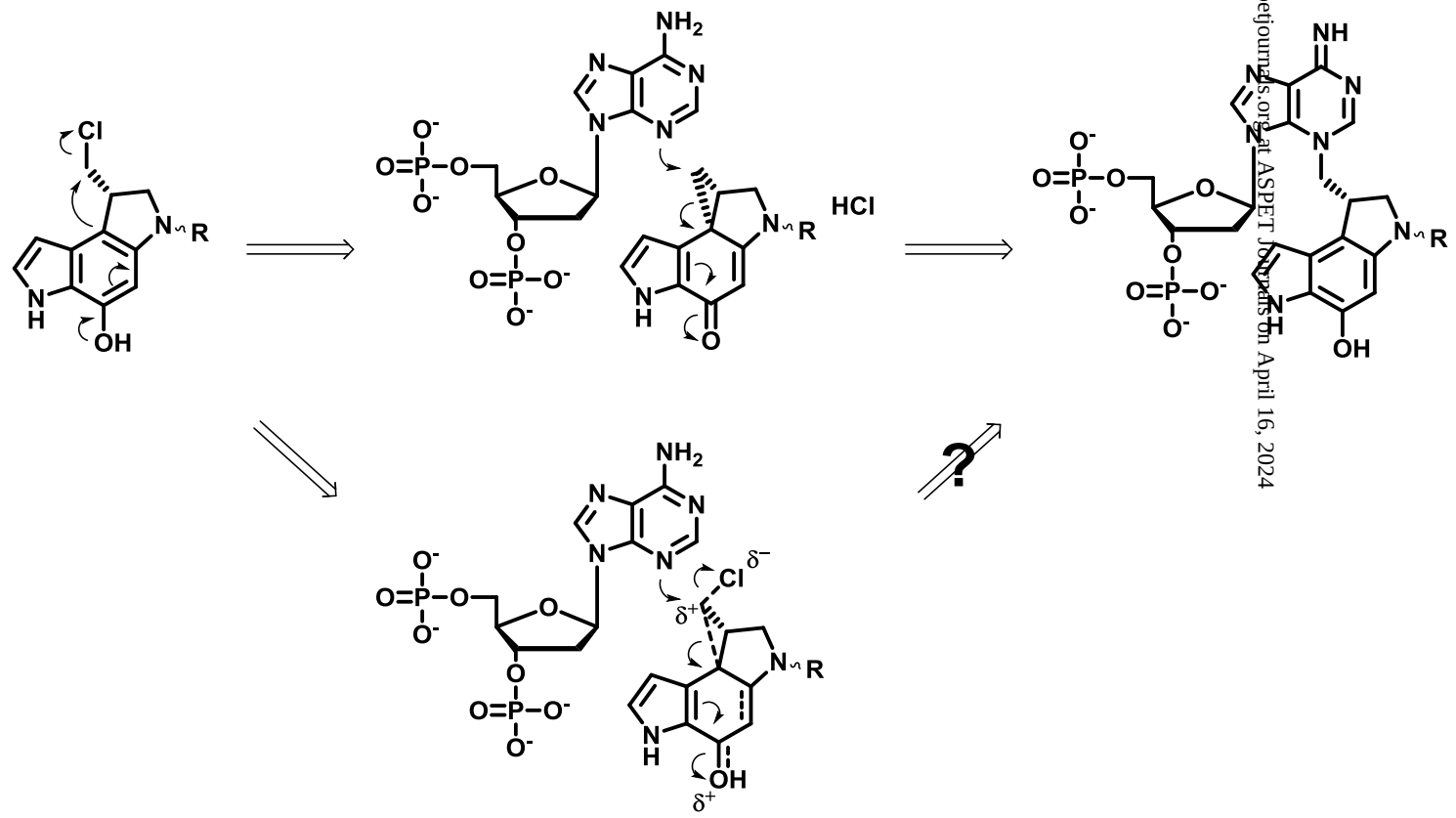

Scheme 2.